3. M. A. Gol'dshtik, T. V. Li, V. M. Khanin, and N. P. Smirnov, Transfer Processes in Chemical Energy Multiphase Systems [in Russian], Novosibirsk (1983), pp. 93-98.
4. Schrage and Perkins, Theoret. Principles of Engineering Computations [Russian translation], No. 1 (1973), pp. 207-213.
5. É. M. Agrest, Symposium on the Physics of Acoustic-Hydrodynamic Phenomena [in Russian], Sukhumi (1975), pp. 45-50.
6. A. S. Dudko, Dokl. Akad. Nauk UkrSSR, Ser. A, No. 4, 77-80 (1989).
7. MacCracken and W. Dorn, Numerical Methods and FORTRAN Programming [Russian translation], Moscow (1977).
8. V. G. Levich, Physicochemical Hydrodynamics [in Russian], Moscow (1959).

LASER PLASMA IN A VACUUM AS AN INTENSE SOURCE OF UV RADIATION

A. P. Golub' and I. V. Nemchinov

UDC 533.951

By using estimates and numerical simulation it is shown that an aluminum plasma sustained by CO_2-laser radiation can radiate intensively in a vacuum in the hard ultraviolet range. High values of the conversion coefficient are achieved for lower radiation flux densities than in the neodymium laser case.

A plasma initiated by a "burst" of absorption [1-3] into disintegrating erosion vapors occurs on the surface of an opaque obstacle in a vacuum under the action of IR band laser radiation. If further action is realized under plane one-dimensional motion conditions, then as the geometric and optical thicknesses of the plasma layer increases a considerable part of the delivered laser energy can be converted into thermal radiation energy emitted by a plasma in a vacuum [4-6]. In that case, when the geometric thickness of the vapor layer becomes commensurate with the characteristic dimension of the spot being irradiated, a self-consistent vapor scattering and heating mode is set up [7-9] because of expansion in the side direction, where the gasdynamic and radiation parameters achievable at the end of the plane stage are maintained by laser radiation at a quasistationary level. Estimates [9-11] and experiments [10-13] show that in this case reradiation can also be a sufficiently substantial factor. Among the distinctive features of a laser plasma in a vacuum should be the possibility of heating it to high enough temperatures to assure emission of radiation of the necessary hardness down to the far vacuum ultraviolet and soft x-ray. The efficiency of plasma heating is increases as the energy of the laser quanta diminishes. Meanwhile, the optical thickness of the plasma heated in a self-consistent mode drops for its intrinsic thermal radiation. It is interesting to investigate how the radiation properties of a laser plasma change here.

The thermal radiation of a plasma was examined in [4-6, 9-13] just for the Nd-laser case. By using estimates and numerical computations the reradiation of an aluminum plasma with characteristic dimension of approximately 1 cm sustained by CO_2-laser radiation at moderate flux densities, namely, $10\text{-}10^4$ MW/cm^2, is investigated in this paper. A comparison is also made with the case of Nd-laser radiation action. Lateral broadening of the plasma jet is simulated by spherically symmetric motion.

1. The plasma energy losses due to its intrinsic thermal radiation are determined by the temperatures achieved therein, the densities, and the characteristic dimensions of the plasma.

O. Yu. Shmidt Institute of Physics of the Earth, Academy of Sciences of the USSR, Moscow. Translated from Inzhenerno-Fizicheskii Zhurnal, Vol. 59, No. 1, pp. 51-61, July, 1990. Original article submitted May 3, 1989.

 0022-0841/90/5901-0852$12.50

We estimate the gasdynamic parameters of an aluminum plasma by using the solution of a spherically-symmetric problem about the stationary mode of vapor dissipation and heating while neglecting reradiation [8]

$$T_m = 21 q_{L0}^{0,331} r_0^{0,168} \varepsilon_L^{-0,338},$$
$$\rho_* = 0{,}063 r_0^{-0,625} \varepsilon_L^{1,25}, \tag{1}$$
$$T_m,\ \text{кК};\ \rho_*,\ \text{mg/см}^3;\ q_{L0},\ \text{MW/cm}^2;\ r_0,\ \text{cm};\ \varepsilon_L,\ \text{eV}.$$

We approximate the magnitude of the spectral absorption coefficient (taking account of emission) due to the braking mechanism and photoeffect by the expressions [14]

$$k_\varepsilon' = \frac{k_L \varepsilon_L^2 kT}{\varepsilon^3}\left(\exp\left(\frac{\varepsilon}{kT}\right) - 1\right) \quad \text{for} \quad \varepsilon < \bar{I},$$
$$k_\varepsilon' = \frac{2k_L \varepsilon_L^2 \bar{I}}{\varepsilon^3}\exp\left(\frac{\bar{I}}{kT}\right)\left(1 - \exp\left(-\frac{\varepsilon}{kT}\right)\right) \quad \text{for} \quad \varepsilon \geqslant \bar{I}, \tag{2}$$
$$\frac{\varepsilon_L}{kT} \ll 1,\ \frac{\bar{I}}{kT} \approx 5,\ k_L(T,\ \rho).$$

The characteristic dimension of a laser plasma is the laser radiation path $L = 1/k_L$. To estimate its radiative properties we consider a plane layer of thickness $L(T, \rho)$ with constant temperature T and density ρ. Using (2) we determing the mean Planck optical thickness of this layer and the flux density of the radiation it emits:

$$\tau_P' = \frac{1}{B}\int_0^\infty \frac{k_\varepsilon'}{k_L} B_\varepsilon d\varepsilon = 2\left(\frac{\varepsilon_L}{kT}\right)^2 \ll 1,$$
$$q_r' = 2\tau_P' B = 4\sigma T^4 \left(\frac{\varepsilon_L}{kT}\right)^2, \tag{3}$$

where

$$B_\varepsilon = \frac{15}{\pi^4}\frac{\sigma\varepsilon^3}{\exp\left(\frac{\varepsilon}{kT}\right) - 1};\quad B = \int_0^\infty B_\varepsilon d\varepsilon = \sigma T^4.$$

Substituting the expression for the quantity T_m from (1) into (3), we find the ratio $\zeta_r' = q_r'(T_m, \varepsilon_L)/q_{L_0}$ characterizing the efficiency of laser energy conversion into plasma brehmsstrahlung and recombination radiation energy

$$\zeta_r' = 1{,}3 q_{L0}^{-0,298} r_0^{0,336} \varepsilon_L^{1,32}, \tag{4}$$
$$q_{L0},\ \text{MW/см}^2,\ r_0,\ \text{cm},\ \varepsilon_L,\ \text{eV}.$$

It follows from the estimates presented that a high-temperature laser plasma is optically transparent for intrinsic brehmsstrahlung and recombination radiation. Photons with energy ε exceeding the running ionization potential $\bar{I}$ introduce the main contribution to the de-excitation energy. The spectrum $\varphi_\varepsilon' = q_\varepsilon'/q_r'$ of the radiation being emitted in a vacuum is a plateau down to the running ionization potential $\bar{I}$, $\varphi_\varepsilon' = 1/3\bar{I}$ for $\varepsilon < \bar{I}$ and furthermore, has an abrupt exponential drop after a jumplike growth: $\varphi_\varepsilon' = \frac{2}{3}\frac{\exp((\bar{I}-\varepsilon)/kT)}{kT}$ for $\varepsilon \geq \bar{I}$.

Let us present an example of calculations by the approximate formulas (1), (3), (4). For CO_2-laser radiation (ε_L = 0.116 eV) for q_{L_0} = 100 MW/cm^2 and r_0 = 1 cm, we obtain T_m = 220 kK, $\tau_P'(T_m) \sim 10^{-4}$, ζ_r' = 0.02. For Nd-laser radiation (ε_L = 1.16 eV) for the same parameters we have T_m = 104 kK, $\tau_P'(T_m)$ = 0.03, ζ_r' = 0.4. Therefore, the braking and photorecombination processes proceeding in the laser plasma with characteristic dimension less than 1 cm will not assure high efficiency of conversion of the CO_2-laser energy delivered to the plasma as well as Nd-laser radiation for flux densities $q_{L_0} > 1$ GW/cm^2 into energy of intrinsic plasma thermal radiation. According to such estimates, a plasma heated by CO_2-laser radiation glows more weakly than for the case of the Nd-laser.

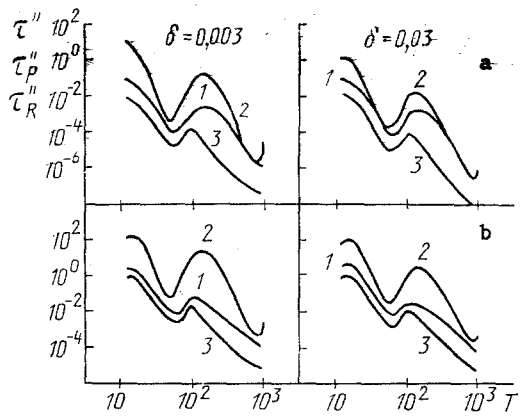

Fig. 1. Mean optical thicknesses τ'', τ_P'', τ_R'' (curves 1, 2, and 3) of a plane aluminum plasma layer heated by CO_2-laser (a) and Nd-laser (b) radiation as a function of the temperature T [kK] for typical values of the relative density δ.

Under conditions of optical plasma transparency in a continuous spectrum, radiation transfer in the lines plays an important part in energy losses. Meanwhile, utilization of assumptions about the total optical transparency in the whole spectrum including near the center of the line, and application of Planck averaging in which the contribution to the magnitude of the volume de-excitation of the quite high values of absorption coefficients at the centers of the lines is again emphasized, can significantly exaggerate the flux of the radiation being emitted.

Let us use the detailed tables [15, 16] of the real optical properties of an aluminum plasma. These tables are compiled with free–free, bound–free, and bound–bound transitions taken into account, contain information about the values of the spectrum coefficients k_ε (T, ρ) at 4600 points on the spectrum located nonuniformly in conformity with the nature of the change in the absorption coefficients, which affords a possibility for an accurate description of both the spectral continuous absorption sections and the numerous line contours in a broad range of temperature T and density ρ.

Let us determine the radiation flux density $q_r''(T, \rho, \varepsilon_L)$ of a plane layer of a laser plasma and its mean optical thickness $\tau''(T, \rho, \varepsilon_L)$ from the relationship

$$q_r'' = \int_0^\infty B_\varepsilon \left(1 - 2E_3\left(\frac{k_\varepsilon}{k_L}\right)\right) d\varepsilon = B\,(1 - 2E_3(\tau'')). \tag{5}$$

Let us also calculate the mean Planck $\tau_P''(T, \rho, \varepsilon_L)$ and Rosseland $\tau_R''(T, \rho, \varepsilon_L)$ optical thicknesses of this layer

$$\tau_P'' = \int_0^\infty \frac{k_\varepsilon}{k_L} B_\varepsilon d\varepsilon / B, \quad \tau_R'' = \frac{\partial B}{\partial T} \Big/ \left(\int_0^\infty \frac{k_L}{k_\varepsilon} \frac{\partial B_\varepsilon}{\partial T}\, d\varepsilon\right).$$

Certain graphical illustrations of the mean optical thicknesses introduced are represented in Fig. 1. Substituting the values of the gasdynamic parameters from (1) into (5), we find the quantity

$$\zeta_r''(q_{L0}, r_0, \varepsilon_L) = q_r''(T_m, \rho_*, \varepsilon_L)/q_{L0}$$

which is an estimate of the efficiency of converting laser radiation into thermal radiation of a plasma (see the graphs in Fig. 2).

It is seen from Fig. 1 that for $kT \gg \varepsilon_L$ a laser plasma is optically transparent ($\tau'' \ll 1$) on the average, however, radiation reabsorption in the lines ($\tau'' \ll \tau_P'$) is essential for it. The line wings introduce the main contribution to the energy being de-excited ($\tau'' \gg \tau_R''$). A "surge" of selective opacity is observed in the T = 90-400 kK temperature range, mean optical thicknesses pass through a maximum. In this temperature range, in the domain of the "radiation barrier" the power of the radiant losses of an aluminum plasma of approxi-

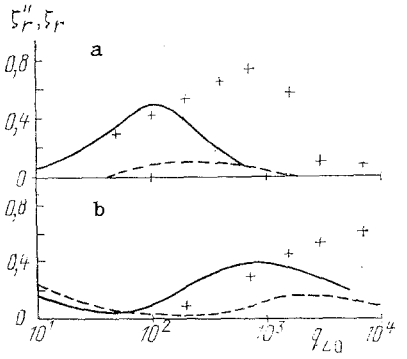

Fig. 2. Efficiency of laser radiation conversion into thermal radiation of an aluminum plasma in the stationary mode as a function of the radiation flux density q_{L_0} [MW/cm^2] of a CO_2-laser (a) and a Nd-laser (b): estimation of the efficiency ζ_r'' for $r_0 = 1$ cm (solid curves), for $r_0 = 0.1$ cm (dashes); values of the efficiency ζ_r (crosses) for $r_0 = 1$ cm obtained during numerical modeling.

mately 1 cm dimension becomes commensurate with the power of the delivered laser energy (Fig. 2), where the efficiency of reradiation from a CO_2-laser plasma turns out to be higher than from a Nd-laser plasma for a laser radiation flux density of $q_{L_0} \sim 100$ MW/cm^2. As the plasma dimension diminishes, the reradiation efficiency drops and its maximum is shifted toward an increase in the laser radiation flux density. The influence of reradiation on the plasma gasdynamic parameters and the presence of layers therein with a different temperature up to the maximal, and a different density possessing different emissivities were not taken into account in the estimates presented. Let us go to numerical computations in which the influence of the opacity of selective radiation is taken carefully into account in the energetic balance.

2. Let us perform the numerical solution of a nonstationary spherically symmetric radiation-gasdynamic problem about the action of laser radiation on an opaque obstacle in a vacuum.

The system of equations describing plasma motion has the form

$$\rho r^2 \frac{\partial r}{\partial m} = 1, \quad \frac{\partial u}{\partial t} = -r^2 \frac{\partial p}{\partial m},$$

$$\frac{\partial e_e}{\partial t} + p_e \frac{\partial}{\partial m}(r^2 u) + \frac{\partial}{\partial m}(F_e + F_r + F_L) = -Q_{ea},$$

$$\frac{\partial e_a}{\partial t} + p_a \frac{\partial}{\partial m}(r^2 u) = Q_{ea}, \tag{6}$$

$$Q_{ea} = \frac{3\nu_{ea}\alpha_e m_e (kT_e - kT_a)}{M}, \quad F_e = -k_e r^2 \frac{\partial T_e}{\partial r},$$

$$p = p_e + p_a, \quad p_e = \frac{\alpha_e \rho k T_e}{M}, \quad p_a = \frac{\rho k T_a}{M}, \quad e_a = \frac{3}{2}\frac{kT_a}{M},$$

$$e_e(T_e, \rho), \ \alpha_e(T_e, \rho), \ \nu_{ea}(T_e, \rho), \ k_e(T_e, \rho),$$

$$0 \leqslant m \leqslant m_w(t), \ t > 0.$$

Propagation of the laser radiation directed along the radii is described in the geometric optics approximation

$$\frac{\partial F_L^{\pm}}{\partial r} = \mp k_L F_L^{\pm}, \tag{7}$$

$$F_L = F_L^- - F_L^+, \ F_L^{\pm} = r^2 q_L^{\pm}.$$

The solution of (7) is continued up to the critical surface (the plasma frequency is commensurate with the laser frequency in its neighborhood), which is joined with the solution of the wave equation by the relationships [17]

$$F_L^+(r_k + 0) = k_k F_L^-(r_k + 0), \tag{8}$$

$$F_L^-(r_k - 0) = (1 - k_k) F_L^-(r_k + 0),$$

$$k_h = \exp\left(-\frac{a\varepsilon_L \varepsilon_d''(r_h)}{\left|\left(\frac{d\varepsilon_d'}{dr}\right)_h\right|}\right), \tag{8}$$

$$\varepsilon_d'(r_h) = 0,\ \varepsilon_d'(T_e,\ \rho,\ \varepsilon_L),\ \varepsilon_d''(T_e,\ \rho,\ \varepsilon_L).$$

The nonequilibrium thermal radiation field is described by the transport equations

$$\frac{\partial I_\varepsilon^\pm}{\partial s} = k_\varepsilon (I_{\varepsilon p} - I_\varepsilon^\pm), \tag{9}$$

$$I_\varepsilon^\pm(t,\ r,\ \mu),\ I_{\varepsilon p}(T_e) = \frac{B_e}{\pi},\ \mu = \cos\theta \geqslant 0.$$

The flux F_r and flux density q_r of the thermal radiation are expressed in terms of the spectral intensity $I_\varepsilon^\pm$:

$$q_r^\pm = 2\pi \int_0^\infty d\varepsilon \int_0^1 I_\varepsilon^\pm \mu d\mu, \tag{10}$$

$$q_r = q_r^- - q_r^+,\ F_r = r^2 q_r.$$

The system of equations (6)-(10) is supplemented by boundary conditions.

On the boundary with the vacuum

$$m = 0,\ p = 0,\ F_e = 0,\ I_\varepsilon^- = 0, \tag{11}$$

$$F_L^- = F_{L0}(t),\ t > 0.$$

The boundary $m_w(t)$ and the conditions thereon are determined as follows.

If the pressure p_c in the obstacle is less than the critical pressure p_{vk} (in the van der Waals sense), then the separation of the substance into condensed and vapor phases is taken into account. The substance in the condensed state is considered incompressible and its heating is determined by ordinary thermal conductivity

$$\rho_c \frac{\partial e_c}{\partial t} - \frac{\partial}{\partial r}\left(k_c \frac{dT_c}{\partial r}\right) = 0,$$

$$e_c = \int_0^{T_c} c_c dT_c + \lambda_{mt} y, \quad \begin{array}{l} y = 0 \text{ for } T_c < T_{mt}, \\ 0 \leqslant y \leqslant 1 \text{ for } T_c = T_{mt}, \\ y = 1 \text{ for } T_c > T_{mt}; \end{array} \tag{12}$$

$$T_c(t=0) = 0,\ T_c(r_1) = 0,\ k_c \frac{\partial T_c}{\partial r}\bigg|_{r_w} = -q_c(t),$$

$$r_w = r_0 - \int_0^t u_c dt,\ c_c(T_c),\ k_c(T_c),$$

$$\left(\frac{k_c t}{\rho_c}\right)^{1/2} \ll r_w - r_1,\ \frac{r_w - r_1}{r_w} \ll 1,\ 0 < r_1 \leqslant r \leqslant r_w,\ t > 0.$$

On the outer boundary r_w of the condensed substance, evaporation occurs in an infinitely narrow jump, an "evaporation wave," a discontinuity of deflagration type [18] with the following continuity relationships of the mass, momentum, and energy flux

$$\rho_c u_c = \rho_w (u_c - u_w),\ \frac{dm_w}{dt} = \rho_c u_c r_w^2,$$

$$p_c + \rho_c u_c^2 = p_w + \rho_w (u_c - u_w)^2, \tag{13}$$

$$-q_c + \rho_c u_c \left(e_c(t,\ r_w) - \lambda_v + \frac{p_c}{\rho_c} + \frac{u_c^2}{2}\right) =$$

$$= -q_w + \rho_c u_c \left(e_{aw} + e_{ew} + \frac{p_w}{\rho_w} + \frac{(u_c - u_w)^2}{2}\right).$$

These relationships hold

$$q_w = q_{Lw}^{-}(1 - k_r) + q_{rw}^{-} + \left(k_e \frac{\partial T}{dr}\right)_w,$$
$$q_{Lm}^{+} = k_r q_{Lm}^{-},\ q_{rw}^{+} = 0,\ T_{c0} = T_c(t,\ r_w),\ k_r(T_{c0}). \tag{14}$$

It is assumed that the phase discontinuity is an isothermal jump with respect to electrons

$$T_{c0} = T_{ew}. \tag{15}$$

It is considered that because of the presence of all possible defects in the real substance, gas inclusions, easily boiling impurities, etc., overheating of the condensed phase is negligibly small and the vapor formation process occurs as a result of equilibrium bulk evaporation. The pressure dependence on temperature on both sides of the evaporation wave for saturated vapors

$$p_c = p_v(T_{c0}),\ p_{aw} = p_v(T_{aw}),\ \text{for}\ u_c > 0\ p_v(T_{c0}) > p_w \tag{16}$$

corresponds to the beginning and termination of the phase transition.

If the saturated vapor pressure at a temperature equal to the surface temperature of the condensed substance is less than the pressure in the plasma, then there is no phase transition and the relationships (13)-(15) and the condition

$$u_c = u_w = 0 \text{ for } p_v(T_{c0}) \leqslant p_w \tag{17}$$

hold on the phase boundary.

The system of equations (6)-(17) describes self-consistent evaporation wave propagation and plasma motion. From the mathematical viewpoint this means that pressure and velocity disturbances transferrable along the characteristics of the gasdynamic equations [19] in a wave exert influence on the evaporation process. If none of the characteristics overtakes the evaporation wave, then the self-consistency condition is disturbed and the Jouget condition should be utilized in this case

$$u_c - u_w = c_w. \tag{18}$$

If the pressure p_c in the obstacle is greater than the critical pressure p_{vk} then the gaseous and condensed states of the substance are not distinct and there is no phase interfacial boundary. However, it is convenient to introduce a conditional plasma boundary m_w in the computations, on which the temperature will equal the critical temperature T_{vk} and to utilize the relationships (13)-(15) for $u_w = u_c = 0$, $k_r = 0$ on this boundary, which would "merge" the gasdynamic problem (6) with the heat conduction problem (12).

Numerical modeling of a laser plasma is realized in two steps. In the first, the time of absorption burst origination for the laser radiation in the erosion vapors is determined by solving (6)-(18) upon the insertion of a heat insulated surface microlayer in the formulation of the problem (12); initiation of a plasma during evaporation of heated surface microdefects in a preferable manner was modeled by such a method [1-3]. In the second step, the problem (6)-(18) is solved anew upon replacement of the gasdynamic distributions from (6) by gasdynamic distributions of the "deflagrating" plasma found in the first step at a time equal to the "burst" time determined in the first step.

The numerical solution was performed by using a three-point implicit difference scheme of heat conduction and a completely conservative difference scheme of gasdynamics [20]. The method of averaging the transport equations [21-23] that permits taking account of the angular directivity and the complex spectrum composition of the radiation in detail was used in the numerical solution. Data were utilized about the thermodynamic [15, 24, 25] and optical [15, 16, 26] properties of aluminum.

3. Let us describe the calculation results. We examine the action of CO_2- or Nd-laser radiation constant in time and directed along the radii on an aluminum spherical obstacle of radius $r_0 = 1$ cm, where the energy flux desnity on the obstacle surface is $q_{L0} = F_{L0}/r_0^2 = 700$ MW/cm^2.

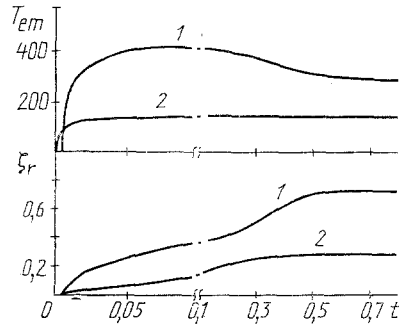

Fig. 3. Dependence of the maximal electron temperature T_{em} [kK] and the reradiation efficiency $\zeta_r = F_{r0}/F_{L0}$ on time t [μsec]. Analysis of the effect of CO_2-laser (1) and Nd-laser (2) radiation on aluminum for $r_0 = 1$ cm, $q_{L0} = 700$ MW/cm^2.

It is seen from Fig. 3 that up to the time t = 0.5 μsec the solutions yield stationary values. In the stationary mode of action the maximal CO_2-laser plasma temperature T_{em} equals 300 kK (1.4 times lower than the estimated value from (1) without taking reradiation into account), while the radiant loss power is 74% with respect to the incident laser energy flux.

For the Nd-laser plasma the reradiation effects turned out to be less strong: De-excitation in a vacuum is 30% in the stationary mode, and reradiation results in a limitation of the maximal temperature at the level T_{em} = 140 kK [T_m = 200 kK according to (1)].

Stationary parameter distributions along the radius r are displayed in Fig. 4. Two domains are distinguished clearly in the temperature profile $T_e(r)$ of the CO_2-laser plasma: The first is the high-temperature domain of the laser torch "corona" in which the flux F_L of laser radiation is absorbed that has not reached the surface with the critical electron concentration, and the second, less hot domain at the obstacle surface and the corona domain forced back from it that is formed due to evaporation of the obstacle and heating of the vapor by the thermal radiation flux F_r. Because of the comparatively weak reradiation for the Nd-laser plasma, the second domain has a considerably smaller size while the laser torch corona is located in direct proximity to the obstacle surface. It follows from the computations that separation of the electron from the ion and atomic temperatures is not large.

Stationary spectra of the radiation emitted into a vacuum are represented in Fig. 5. The radiation spectrum of the CO_2-laser plasma (Fig. 5a) graphically demonstrates the high degree of selectivity of the radiation. Lines exceeding the photorecombination continuum level by 2-4 orders play the principal role therein. The role of the lines is not so significant in the radiation spectrum of the Nd-laser plasma, which agrees with the estimates of Sec. 1. Let us examine the contribution of individual sections of the spectrum (photon groups) to de-excitation by denoting the relative contribution of the first group ($\varepsilon < 6$ eV) to the total energy flux F_{r_0} radiated in the vacuum by η_{r1}, by η_{r2}, η_{r3}, η_{r4} their relative contributions of the second ($\varepsilon < 30$ eV), third (30 eV $\leq \varepsilon \leq$ 100 eV), and fourth ($\varepsilon >$ 100 eV) groups. We have η_{r1} = 0.4%, η_{r2} = 3%, η_{r3} = 58%, η_{r4} = 39% for F_{r0} = 520 MW/sr in the CO_2-laser plasma spectrum. The spectrum of the Nd-laser plasma is less hard: η_{r1} = 3%, η_{r2} = 22%, η_{r3} = 63%, η_{r4} = 15%, F_{r0} = 210 MW/sr.

It should be noted that for typical values of the parameters, T_e = 300 kK, δ = 0.01 the ionization time of the triple aluminum ion by electron impact from the ground state is 0.07 μsec [27], which is an order less than the characteristic time of the problem. This estimate only justifies to a certain degree the assumption about the equilibrium ionization composition of the plasma and the equilibrium population at the levels in the formulation of the problem. Possible nonequilibrium effects should later be investigated in greater detail.

Computed stationary values ζ_r of the laser plasma reradiation efficiency in a vacuum are noted by crosses in Fig. 2 as a function of the laser radiation flux density q_{L0} on the surface of a spherical aluminum obstacle of radius r_0 = 1 cm. It is seen that the CO_2-laser plasma reradiates more effectively than the Nd-laser plasma in the range of values q_{L0} = 10-10^3 MW/cm^2. The maximum of the coefficient of laser radiation conversion into thermal plasma radiation is achieved at q_{L0} = 700 MW/cm^2 for the CO_2-laser and for $q_{L0} >$ 10 GW/cm^2 for the ND-laser.

NOTATION

r_0, radius of the spherical obstacle; q_{L0}, laser radiation flux density on the obstacle surface in the absence of a plasma; ε_L, energy of laser quanta; T_m, maximal temperature

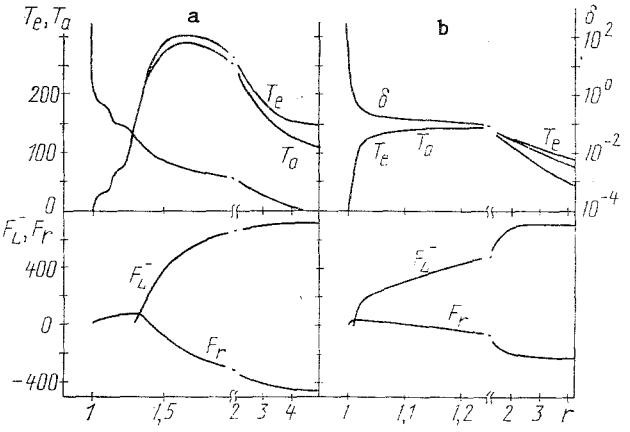

Fig. 4 Distributions of the parameters T_e[kK], T_a[kK], , F^-[MW/sr] along the radius r[cm] at the time t = 0.8 usec in an aluminum plasma heated by CO_2-laser (a) and Nd-laser (b) radiation.

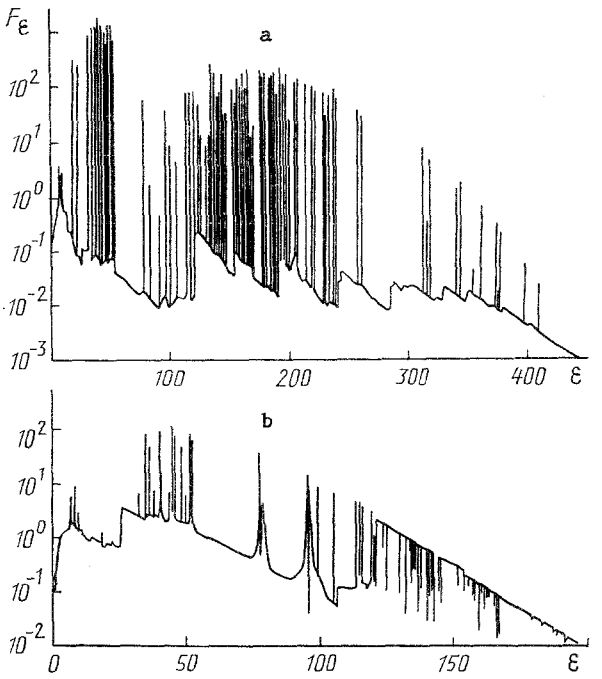

Fig. 5. Spectrum flux F_ε [MW/(sr.eV)] emerging into the thermal radiation vacuum of an aluminum plasma sustained by CO_2-laser radiation (a) and Nd-laser radiation (b) as a function of the photon energy ε [eV] at the time t = 0.8 μsec corresponding to the gasdynamic parameters (see Fig. 4).

achievable in a section close to the sonic; ρ_*, density in a sonic section; k_ε', a quantity approximating the spectral coefficient of radiation absorption due to a brehmsstrahlung mechanism and photoeffect; ε, photon energy; k_L, brehmsstrahlung absorption coefficient for laser radiation; T, temperature; k, Boltzmann constant; ρ, density; ρ_n, normal density corresponding to the Loschmidt number; $\delta = \rho/\rho_n$, relative density; $\bar{I}$, running ionization potential; L, laser radiation mean free path; B_ε and B, spectral and the integral over the spectrum equilibrium radiation flux densities of an absolutely black body; σ, Stefan–Boltzmann constant; τ_P', q_ε', and q_r', estimates of the mean Planck optical thickness, the spectral, and the integral over the spectrum brehmsstrahlung and recombination radiation flux densities of a laser plasma; ζ_r', estimate of the efficiency of laser radiation conversion into brehmsstrahlung and recombination radiation of a plasma; φ_ε', estimate of the spectrum of plasma-emitted brehmsstrahlung and recombination radiation; k_ε, spectral absorption coefficient with free–free, bound–free, and bound–bound transitions taken into account; τ'', τ_P'', τ_R'', q_r'', estimates of the mean true, Planck, Rosseland optical thicknesses of a plane laser layer, the flux density of the thermal radiation emitted by this layer; E_3, integral exponent; ζ_r'', estimate of the efficiency of laser radiation energy conversion into plasma thermal radiation energy; t, time; m, Lagrange mass variable; m_w, plasma mass per unit solid angle; r, Euler coordinate; u, velocity; T_e, temperature of the electron subsystem consisting of free and bound electrons; T_a, atom–ion subsystem temperature; p_e, p_a, p, partial and total pressures; e_e, electron subsystem energy per unit plasma mass, including the thermal motion energy of free electrons and excitation and ionization energy of atoms and ions; e_a, specific thermal motion energy of atoms and ions; Q_{ea}, rate of energy exchange between subsystems; ν_{ea}, frequency of free electron collisions with atoms and ions; α_e, degree of ionization; M, atom (ion) mass; m_e, electron mass; k_e, coefficient of electron heat conductivity; F_e, F_r, F_L, energy fluxes due to electron heat conductivity, thermal radiation, laser radiation; quantities referring to photons being propagated in the positive (negative) direction of the r axis are marked by a plus (minus) superscript; $q_L^\pm$, unilateral density of the laser radiation flux; r_k, critical surface coordinate; k_k, reflection coefficient of laser radiation from the critical surface; ε_d' and ε_d'', real and imaginary parts of the complex dielectric permittivity of the plasma; $(d\varepsilon_d'/dr)_k$, value of the derivative for $r = r_k$; a, a constant; ds, length element along the direction of photon motion; θ, angle of ray intersection with the radius; $I_\varepsilon^\pm$, radiation spectral intensity; $I_{\varepsilon p}$, equilibrium intensity;

$q_r^{\pm}$, unilateral thermal radiation flux density; $F_{L_0}(t)$, a function governing the laser pulse shape; condensed substance parameters are marked with the subscript c; c_c, specific heat; k_c, heat conduction coefficient; T_{c0}, temperature of the evaporating surface; p_v, saturated vapor pressure; p_{vk} and T_{vk}, pressure and temperature at the critical point (in the van der Waals sense); λ_{mt}, latent heat of fusion; λ_v, specific evaporation energy; r_1, radius of the conditional boundary within the obstacle; r_w, radius of the outer boundary of the condensed substance; u_c, velocity of evaporation wave for condensed substance; q_c, energy flux density diverted from the evaporation wave by the heat conduction mechanism for heating and condensed substance; vapor parameters behind the evaporation wave from the vapor; k_r, laser radiation reflection coefficient from the outer boundary of the condensed substance; c_w, sound speed behind the evaporation wave; T_{em}, maximum electron temperature; F_{r0}, plasma thermal radiation flux in a vacuum; ζ_r, reradiation efficiency in a vacuum computed in the numerical modeling of the laser plasma; F_ε, spectral flux of radiation emitted by the plasma in a vacuum; η_{r1}, η_{r2}, η_{r3}, η_{r4}, relative contributions of groups of photons to the total flux of energy being de-excited in a vacuum.

LITERATURE CITED

1. A. P. Golub' and I. V. Nemchinov, Kvantovaya, Élektron., 7, No. 1, 209-211 (1980).
2. A. P. Golub' and I. V. Nemchinov, Kvantovaya, Élektron., 7, No. 8, 1831-1834 (1980).
3. A. P. Golub', I. M. Nemchinov, A. I. Petrukhin, et al., Zh. Tekh. Fiz., 51, No. 2, 316-323 (1981).
4. V. I. Bergel'son and I. V. Nemchinov, Zh. Prikl. Mekh. Tekh. Fiz., 37, No. 2, 236-242 (1973).
5. V. I. Bergel'son and I. M. Nemchinov, Kvantovaya Élektron., 7, No. 11, 2356-2361 (1980).
6. A. V. Dobkin and I. V. Nemchinov, Zh. Prikl. Spektrosk., 38, No. 6, 732-736 (1983).
7. I. V. Nemchinov, Prikl. Mat. Mekh., 31, No. 2, 300-319 (1967).
8. T. B. Malyavina and I. V. Nemchinov, Zh. Prikl. Mekh. Tekh. Fiz., No. 5, 58-75 (1972).
9. A. V. Dobkin, T. B. Malyavina, and I. V. Nemchinov, Zh. Prikl. Mekh. Tekh. Fiz., No. 1, 3-11 (1988).
10. N. G. Basov, G. A. Vergunov, P. P. Volosevich, et al., Kvantovaya Élektron., 14, No. 9, 1887-1893 (1987).
11. A. P. Bolub', A. V. Dobkin, and I. V. Nemchinov, Izv. Akad. Nauk SSSR, Ser. Fiz., 52, No. 9, 1817-1825 (1988).
12. V. I. Artem'ev, S. A. Medvedyuk, I. E. Markovich, et al., Izv. Akad. Nauk SSSR, Ser. Fiz., 52, No. 9, 1861-1863 (1988).
13. V. I. Bayanov, A. P. Golub', V. A. Gorbunov, et al., Izv. Akad. Nauk SSSR, Ser. Fiz., 53, No. 3, 480-485 (1989).
14. Ya. B. Zel'dovich and Yu. P. Raizer, Shock Wave Physics and High-Temperature Gasdynamic Phenomena [in Russian], Moscow (1966).
15. V. P. Buzdin, A. V. Dobkin, and I. B. Kosarev, Thermodynamic and Optical Properties of a High-Temperature Plasma [in Russian], Dep. No. 52-84, VINITI, Moscow (1984).
16. A. V. Dobkin, I. B. Kosarev, and I. V. Nemchinov, Optical Properties of High-Temperature Aluminum Plasma [in Russian], Dep. No. 4220-83, VINITI, Moscow (1983).
17. V. L. Ginzburg, Electromagnetic Wave Propagation in a Plasma [in Russian], Moscow (1967).
18. S. I. Anisimov, Ya. A. Imas, G. S. Romanov, and Yu. V. Khodykov, Action of Laser Radiation of High Power on Metals [in Russian], Moscow (1970).
19. R. Courant and K. Friedrichs, Supersonic Flow and Shock Waves [Russian translation], Moscow (1950).
20. A. A. Samarskii and Yu. P. Popov, Gasdynamics Difference Schemes [in Russian], Moscow (1975).
21. I. V. Nemchinov, Prikl. Mat. Mekh., 34, No. 4, 706-722 (1970).
22. A. P. Golub', Zh. Vychisl. Mat. Mat. Fiz., 23, No. 1, 142-151 (1983).
23. A. P. Golub', Analysis of Dissipation in a Vacuum of a Radiating Aluminum Plasma Heated by Co_2-Laser Radiation by the Method of Averaging the Transport Equations [in Russian], Dep. No. 8066-B86, VINITI, Moscow (1986).
24. V. B. Glushko, L. V. Gurvich, G. A. Bergman, et al. (eds.), Thermodynamic Properties of Individual Substances (Handbook) [in Russian], Moscow (1962).
25. I. K. Kikoin (ed.), Tables of Physical Quantities (Handbook) [in Russian], Moscow (1976).

26. K. Ujihara, J. Appl. Phys., 43, No. 5, 2376-2383 (1972); IEEE, J. Quant. Electron., QE-8, No. 6, 567-568 (1972).
27. L. A. Vainshtein, I. I. Sobel'man, and E. A. Yukov, Atom Excitation and Spectrum Line Broadening [in Russian], Moscow (1979).